

Periodic Anderson Model with Holstein Phonons for the Description of the Cerium Volume Collapse

Enzhi Li^{1,2}, Shuxiang Yang^{1,2}, Peng Zhang³, Ka-Ming Tam^{1,2}, Mark Jarrell^{1,2}, and Juana Moreno^{1,2}

¹ *Department of Physics & Astronomy, Louisiana State University, Baton Rouge, LA 70803, USA*

² *Center for Computation & Technology, Louisiana State University, Baton Rouge, LA 70803, USA and*

³ *Department of Physics, Xi'an Jiaotong University, Xi'an, Shaanxi, China*

(Dated: April 18, 2022)

Recent experiments have suggested that the electron-phonon coupling may play an important role in the $\gamma \rightarrow \alpha$ volume collapse transition in Cerium. A minimal model for the description of such transition is the periodic Anderson model. In order to better understand the effect of the electron-phonon interaction on the volume collapse transition, we study the periodic Anderson model with coupling between Holstein phonons and electrons in the conduction band. We find that the electron-phonon coupling enhances the volume collapse, which is consistent with experiments in Cerium. While we start with the Kondo Volume Collapse scenario in mind, our results capture some interesting features of the Mott scenario, such as a gap in the conduction electron spectra which grows with the effective electron-phonon coupling.

I. INTRODUCTION

The isostructural volume collapse of Cerium is a long-standing puzzle [1]. When a crystal of Cerium is under a pressure of 15,000 atmospheres, it undergoes a volume collapse of approximately 17% while preserving the face-centered cubic crystal structure. This transformation, called the $\gamma \rightarrow \alpha$ transition, has baffled physicists since its discovery, and several leading theories have been proposed for its explanation, the most prominent of which are the Mott transition scenario [2] and the Kondo volume collapse (KVC) scenario [3]. The Mott and KVC scenarios are competing paradigms, although perhaps not as different and distinct as previously thought [4, 5].

In the KVC scenario, the $4f$ electrons of Cerium are assumed to be localized in both phases. In the small volume α phase, the spd electrons strongly screen the local moments of the f electrons, thus rendering the α phase a Pauli paramagnet. While in the large volume γ phase, the local moments of the f electrons persist to much lower temperatures than in the α phase, indicating that the Kondo scale T_K in the γ phase is much smaller than that of the α phase, which is consistent with the experimental observations [6–9].

In the Mott transition scenario, for which the Hubbard model is a good description, the density of states (DOS) of the f electrons changes from being metallic (no gap at the Fermi level) in the α phase to insulating (with a gap at the Fermi level) in the γ phase [5, 10–12]. This localization-delocalization of the $4f$ electrons, which is a metal-insulator Mott transition, is driven by the increase of the intersite hopping amplitudes of the f electrons when the unit cell volume of Cerium decreases.

While there are extensive studies on the cerium volume collapse, there is no consensus on the mechanism of this transition. An overview on the cerium volume collapse can be found in Ref. [13]. Most of the previous models proposed consider exclusively the interplay among the spd electrons and the f electrons, whereas the possible effects from the phonons are completely ignored. A se-

ries of recent experimental results have indicated that the electron-phonon interaction may also play an important role in the $\gamma \rightarrow \alpha$ transition [14–17]. Jeong *et al.* [17] estimated that about one half of the entropy change during the transition is due to lattice vibrations. Later, Krisch *et al.* [15] showed that the significant changes in the phonon dispersion across the $\gamma \rightarrow \alpha$ transition provide strong evidences for the importance of the lattice degrees of freedom. Although the precise value of the lattice vibrational entropy varies between experiments, they do agree that a significant fraction of the total entropy change during the transition is due to lattice vibrations. This calls for a revision of the previous models to incorporate the contribution from the electron-phonon coupling.

Even if we focus exclusively on the electronic contribution, the full model should be more complicated than the simple single band Periodic Anderson model or Hubbard model. Recent studies have refined the theoretical modeling by the density functional theory. These studies have confirmed that the $f - spd$ hybridization is important [18–22], while for a quantitative description the spin-orbit coupling of the f electrons and the hybridization among the f orbitals are two other contributions which should be taken into account [23, 24].

The obtained band structure can be fed into other methods which can reveal physics from strong coupling which is presumably absent from the DFT, such as Kondo effect and Mott transition. These methods included dynamical mean field theory (DMFT), [5, 22, 24–28], variational Monte Carlo [29], and Gutzwiller projection approach [28, 30]. Constrained Random Phase Approximation can be further used to estimated the coupling terms [24, 31].

Unfortunately, there is no well developed method to incorporate the electron-phonon interaction into this framework. Moreover there is no appropriate formalism to include dynamical phonons with non-trivial dispersions within the DMFT, as it will involve effective non-local electron-electron interaction. A quantitative study of electron-phonon coupling with the accuracy on

par with that of the pure electron-electron coupling is the ultimate goal but not practically feasible at present. In light of these difficulties on the modeling of electron-phonon coupling, we sought for a model which is simple enough to handle by numerics and nevertheless capture the first order transition. Electron-phonon is then incorporated into the model and its effect can be studied in some details.

So as to attain the above goal we consider the contribution of phonons within the Kondo volume collapse scenario, this is in line of the original approach by Allen and Martin [3]. They studied the contributions of the free energy from the electronic part and the bulk modulus. In their study, the electronic part is modeled by a single impurity model. In this work, we use the periodic Anderson model with Holstein phonons coupled to the conduction band as our starting point [32]. We solve this model using the DMFT approximation with the continuous time quantum Monte Carlo as our impurity solver. We then use the maximum entropy method to extract the density of states (DOS) of the conduction electrons, and study the evolution of DOS with varying parameters.

Our main finding is that the electron-phonon interaction can significantly enhance the volume collapse of the Cerium under our model frame-work, and associated with this volume collapse, a metal-insulator transition emerges. Although we start our model with the Kondo scenario in mind, yet a Mott metal insulator transition that manifests itself by a gap formation is observed. Thus, our work may pave the way for the unification of the competing Kondo and Mott scenarios, a unification that is already lurking in the previous works [4, 5].

The structure of the paper is as follows. In section II, we give our model Hamiltonian and briefly describe the methods we use to solve our model. In section III, we present our results for the pressure-volume curves, the behavior of the DOS across the phase transition, and discuss the relationship between the volume collapse and the Mott transition. We make a conclusion in section IV.

II. MODEL AND METHOD

In order to study the influence of the phonons on the Cerium volume collapse, we have here employed the periodic Anderson model with electron-phonon interactions, which is

$$\begin{aligned} \hat{H} &= \hat{H}_0 + \hat{H}_I \quad (1) \\ \hat{H}_0 &= -t \sum_{\langle i,j \rangle, \sigma} (c_{i,\sigma}^\dagger c_{j,\sigma} + c_{j,\sigma}^\dagger c_{i,\sigma}) + \epsilon_f \sum_{i,\sigma} f_{i,\sigma}^\dagger f_{i,\sigma} \\ &\quad + V \sum_{i,\sigma} (c_{i,\sigma}^\dagger f_{i,\sigma} + f_{i,\sigma}^\dagger c_{i,\sigma}) + \sum_i \left(\frac{P_i^2}{2m} + \frac{1}{2} k X_i^2 \right) \\ \hat{H}_I &= U \sum_i n_{i,\uparrow}^f n_{i,\downarrow}^f + g \sum_{i,\sigma} n_{i,\sigma}^c X_i. \end{aligned}$$

where $c_{i,\sigma}^\dagger, c_{i,\sigma} (f_{i,\sigma}^\dagger, f_{i,\sigma})$ creates and destroys a $c(f)$ electron of spin σ at lattice site i , respectively. P_i and X_i are the phonon momentum and displacement operators. Here, we have used dispersionless Einstein phonons with frequency $\Omega_0 = \sqrt{k/m}$. The parameter g measures the electron-phonon interaction strength, U is the Hubbard repulsion between localized f -electrons, and V characterizes the hybridization between conduction- and f -electrons. From the parameters g, k , we construct the effective electron-phonon interaction strength, $U_{eff} = \frac{g^2}{2k}$. Throughout this paper and to be consistent with the experimental results, we have set $\Omega_0 = 0.01$ [32] unless otherwise specified. To preserve the large temperature metallic phase, we fix the total electronic density at $n = 1.8$ by tuning the chemical potential at each iteration of the DMFT cycle. We also adjust ϵ_f so that $n_f = 1$ when $T = 0.1$ to ensure that a local moment is present at high temperature. We set $U = 4$, but the precise value of U is not crucial as we have found qualitatively similar results for other values of U .

We propose this simplified model as our first attempt to incorporate the electron-phonon interaction into the study of the Cerium volume collapse. We neglect the Hubbard repulsion in the c -band because it is much smaller than the Hubbard repulsion in the $4f$ band. Amadon and Gerossier [26] found that the value of the inter-site hopping between $4f$ electrons is less than a third of the value of the hybridization between $4f$ and conduction electrons. We neglect the $4f$ -electron inter-site hopping in our model Hamiltonian. The goal is to construct a minimal model which possesses Kondo effect and investigate the influences from electron-phonon coupling.

While this model may not provide a description of cerium in a quantitative manner. The model is already rather complicated and is interesting by itself as it deals with an important class of problems on the effect of impurity models under correlated conduction band [33–36] and have not been extensively studied in the literatures largely due to its complexity. It is particularly challenging with the correlated conduction band due to the electron-phonon coupling [32]. The competition and cooperation among the Kondo effect, Ruderman-Kittel-Kasuya-Yosida coupling, and the correlation effect in the conduction band can lead into a very rich phase diagram [34–36].

With the goal of understanding the volume collapse transition, in this work we will focus exclusively on the Kondo regime in the periodic Anderson model and investigate the effect under the electron-phonon coupling in the conduction band. In particular we will calculate the total free energy to construct the phase diagram and demonstrate the first order transition. In the end, we find that even though our electronic model corresponds to the Kondo volume collapse scenario, the introduction of a phononic coupling with the conduction electrons induces several interesting phenomena reminiscent of the Mott transition.

The model is solved by using the dynamical mean field theory [37], with the continuous time quantum Monte Carlo [38] as our impurity solver. We use a hypercubic lattice with Gaussian bare DOS, and consider its bandwidth as our unit of energy. We set this unit to be the Fermi energy ϵ_F of Cerium, which is 0.52eV [39, 40]. There is no sharp feature in the DOS near the Fermi surface of the cerium, such as flat band or isolated van Hove singularity, therefore it is unlikely the choice of the DOS will affect our goal of investigating the qualitative effect from the electron-phonon coupling. Finally, we use the maximum entropy method [41] to extract the spectral functions from the Monte Carlo simulation data.

III. RESULTS

In the following subsection we draw the pressure-volume (p - \mathcal{V}) phase diagram by calculating the total free energy including the contribution from the bulk modulus. We find that the first order phase transition emerges when the electron-phonon interaction is large. For a fixed set of parameters we employed, the first order transition does not exist even at much lower temperature in the absence of electron-phonon coupling.

After constructing the phase diagram, we investigate the phase transition in more detail by calculating the spectral function of the conduction band across the phase transition. Although we employ the periodic Anderson model, the paradigm for the KVC scenario, our results display features of a Mott transition in the conduction band due to the electron-phonon coupling. In the parameter regime where V is small, as U_{eff} increases, the DOS of the c -electrons gradually develops a gap at the Fermi level with a width proportional to U_{eff} . The gap-opening in the DOS, and its proportionality to U_{eff} mimics that of the Mott transition in the Hubbard model. The gap does not occur when V dominates over U_{eff} , which compels us to argue that there is a competition between V and U_{eff} in our model [42].

A. Bulk Modulus and the Pressure-Volume Diagram

Since the $\gamma \rightarrow \alpha$ transition is first order, the pressure versus volume curve develops a kink as the temperature drops below the transition point. To properly account for the static lattice contribution, we introduce a volume and temperature dependent bulk modulus term into the $p - \mathcal{V}$ relation [3]. Therefore, the total pressure contains two parts, the pressure due to the electrons which we denote as p_e , and the pressure due to the bulk modulus term which we denote as p_B .

We calculate p_e from the electronic free energy by the relation $p_e = -\frac{\partial F}{\partial \mathcal{V}}$, and p_B by integrating the bulk modulus $B = -\mathcal{V} \frac{\partial p_B}{\partial \mathcal{V}}$. We calculate the electronic free energy using the formula $F_e(T = T_0, \mathcal{V} = \mathcal{V}_0, N) =$

$\int_0^N \mu dN + F(T_0, \mathcal{V}_0, N = 0)$. Here, we choose not to use the entropy formula employed in Ref. [43] because the statistical error in our results become large at high temperatures. When we plot the free energy versus hybridization V , we notice that the curve continuously evolves from a nearly flat plateau at small V to a nearly straight line with a negative slope at large V . With this observation, we conjecture that the derivative of the free energy with respect to V can be approximately fitted to the function $-k(1 + \tanh a(V - c))$, with k, a, c being positive parameters. Integration of the derivative gives a function to which we can fit our free energy data:

$$F_e(V) = -k \left(V - c + \frac{1}{a} \log 2 \cosh a(V - c) \right) + d. \quad (2)$$

By fitting our numerical data to Eq. [2], we obtain the values of the parameters k, a, c, d . Since the free energy depends on the temperature, these parameters also depend on it. Now, we can obtain the volume dependence of the free energy using the empirical relationship between hybridization V and volume \mathcal{V} , $V = \frac{b}{\mathcal{V}^2}$ [44]. We calculate the electronic pressure as

$$p_e = -\frac{2kb}{\mathcal{V}^3} \left(1 + \tanh a \left(\frac{b}{\mathcal{V}^2} - c \right) \right). \quad (3)$$

The experimental value of b can be estimated from the relation $V = \frac{b}{\mathcal{V}^2}$, and $J \propto \frac{V^2}{U}$ [45], where J is the Kondo exchange. The experimental values of J range between 0.2 – 0.3eV in the α phase and 0.05 – 0.06eV in the γ phase [6–8, 39]. From the values of J and the relation between J and the volume, we can estimate the value of b to be between 0.89 and 1.55 in our unit system.

The second contribution to the total pressure comes from the bulk modulus. From the experimental results of Ref. [46, 47], we assume that the bulk modulus depends upon the volume as

$$B = B_0(T) e^{\alpha(1-\mathcal{V}/\mathcal{V}_0)}, \quad (4)$$

and upon the temperature through the relation [48]

$$B_0(T) = B_0 \left(1 + e^{-\frac{T_0}{T}} \right), \quad (5)$$

where, B_0, T_0, \mathcal{V}_0 and α are material-dependent parameters.

Integration of the bulk modulus gives us the pressure p_B as

$$p_B(\mathcal{V}, T) = p_0(T) - B_0(T) \int_1^{\mathcal{V}/\mathcal{V}_0} dx \frac{e^{\alpha(1-x)}}{x}, \quad (6)$$

where $p_0(T)$ is an arbitrary constant that may depend on the temperature. Throughout the paper, we have set $p_0 = 0$.

Adding the bulk modulus and the electronic pressures yields a $p - \mathcal{V}$ graph which exhibits a kink structure. Fig. 1 shows the pressure versus volume diagrams for different values of U_{eff} . When $U_{eff} = 1$, as we lower the temperature, a kink structure begins to develop. We

identify $\beta = 6$ as the critical temperature where the kink structure begins to emerge. Experimentally, the ratio between the $\gamma \rightarrow \alpha$ transition critical temperature T_c and the temperature T' where the volume collapse of 17% occurs is $T_c/T' = 460/334$ [49]. Using the same ratio, we can identify the T' in our model to be approximately $1/8$. From the iso-thermal $p - \mathcal{V}$ diagrams, we find that the volume collapse in our model at $\beta = 8$ is about 30%, a result that is in reasonable agreement with the experiments, considering that we are using a highly simplified model. From the Maxwell construction, we can read off from the $\beta = 8$ iso-thermal line the volumes for the γ and α phases, with $\mathcal{V}_\alpha = 0.78$, and $\mathcal{V}_\gamma = 1.13$. We further estimate the corresponding hybridization value for these two phases to be $V_\alpha = 1.93$, and $V_\gamma = 0.92$.

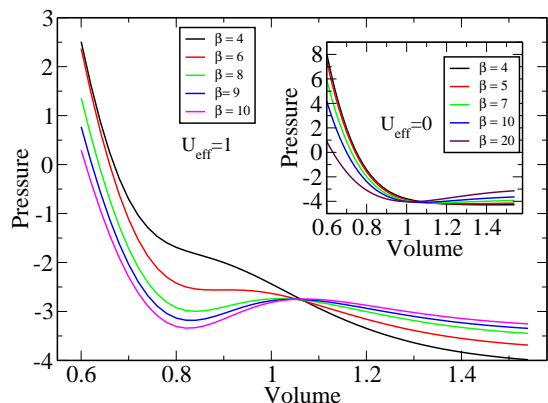


FIG. 1. Main panel: The $p(\text{pressure}) - \mathcal{V}(\text{volume})$ diagram for $U_{eff} = 1, \Omega_0 = 0.01$. As the temperature decreases (critical temperature $T_c = 1/6$), a kink structure develops in the $p - \mathcal{V}$ graph, indicating the emergence of a first order phase transition. Inset: $p - \mathcal{V}$ diagram for $U_{eff} = 0$. Here, with the same bulk modulus pressure, the kink structure does not show up.

On the other hand, when $U_{eff} = 0$ (inset on Fig. 1), even though we have used the same set of parameters, the kink structure that is the indicator for the emergence of a first order phase transition is absent. Note that the small upturn in the $p - \mathcal{V}$ diagram at large volume can also be eliminated once we consider the volume dependence for the hopping term t in the conduction band.

Similar results can be obtained with many different combinations of parameters. In the data displayed in Fig. 1 we set $b = 1.18, p_0 = 0, T_0 = 0.1, B_0 = 12.47$, and $\alpha = 4.225$. The value of b is within our estimated range. A value of $T_0 = 0.1$ is approximately 600 K within our units, a value comparable to the critical point temperature of the transition. Following Ref. [3], we use $B_0 = 28 \text{ GPa}, \mathcal{V}_0 = 36 \text{ \AA}^3$ as the bulk modulus and unit cell volume for Cerium in the γ phase. Once we use the Fermi scale as our unit of energy and set \mathcal{V}_0 as our unit of volume, the unit of pressure becomes $\epsilon_F/\mathcal{V}_0 = 2.3 \text{ GPa}$. This justifies our usage of the value $B_0 = 12.47$ as our

bare bulk modulus. And, finally, the experimental values of α range between 2 and 5 for most bulk pure metals [46].

In summary, for a large range of parameters, if the electron-phonon coupling ($U_{eff} = 1$) is finite, there is a clear first order transition in the $p - \mathcal{V}$ diagram with a critical temperature around $1/6$. However, for the same set of parameters, when the electron-phonon interaction is absent ($U_{eff} = 0$), the transition is not seen for temperatures down to $1/20$. The different behavior of the $p - \mathcal{V}$ diagram for $U_{eff} = 0$ and $U_{eff} = 1$ implies that the electron-phonon interaction enhances the $\gamma \rightarrow \alpha$ volume collapse transition.

B. Spectral Functions of the Mott Metal-Insulator Transition

The phonon-enhanced first order phase transition can be interpreted as a Mott metal-insulator transition. We can understand this by studying the evolution of the spectral functions with respect to the variation of the relative strengths of V and U_{eff} . When the hybridization is small, the electron-phonon interaction can significantly modify the density of states (DOS) of the conduction electrons. For $V = 0.1$, as U_{eff} increases from 0 to 1.1, the DOS changes from a nearly Gaussian to a DOS gapped at the Fermi energy, as shown in Fig. 2. The gap in the conduction electron spectral function is not an artifact of the maximum entropy method since we can also see the effect of U_{eff} on the gap at the Fermi energy by observing the behavior of the local c -electron Green's function $G_c(\tau)$ (inset of Fig. 2), which is directly measured in the Monte Carlo simulation. When there is no gap, the value of $G_c(\tau = \beta/2)$ is finite. However, when there is a gap at $\omega = 0$, the value of $G_c(\tau = \beta/2)$ decays to zero exponentially. Moreover, the wider the gap, the more rapid the decay. When we plot the $G_c(\tau)$ for different values of U_{eff} , we see clearly that with increasing U_{eff} , $G_c(\tau)$ decreases increasingly rapidly when τ approaches $\beta/2$.

The magnitude of the phonon frequency Ω_0 and the c -electron filling have profound influences on the nature of the Mott transition due to U_{eff} . When Ω_0 is small, which is the case we are studying, the transition seems to be continuous or at most weakly discontinuous [50]. The reason is that when $\Omega_0 = 0$, we can integrate out the Holstein phonons to obtain the Falicov-Kimball model in which the conduction electrons always exhibit a non-Fermi liquid behavior for any non-trivial filling number [51, 52]. The Mott transition from a non-Fermi liquid metal to an insulator is continuous due to the absence of the quasi-particle peak at the Fermi energy in the conduction electron DOS [53]. Notice here we are considering only the transition in the electron-phonon system solely from Eq. 1. By including the static lattice contribution this transition becomes first order as we discussed earlier.

The low phonon frequency is chosen in this study because of the low Debye temperature observed in exper-

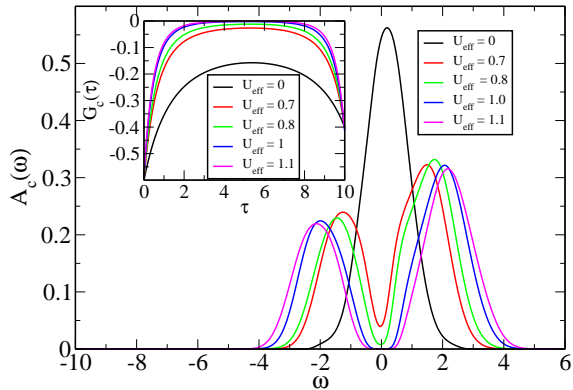


FIG. 2. Main panel: The conduction electron spectral functions for $V = 0.1, \beta = 10, \Omega_0 = 0.01$. As U_{eff} increases from 0.0 to 1.1, the gap in the DOS becomes increasingly wider. Inset: The evolution of the local conduction electron Green's function $G_c(\tau)$ with U_{eff} . The increasingly rapid decay of $G_c(\tau = \beta/2)$ also indicates the existence of an energy gap at $\omega = 0$ as U_{eff} grows.

iments [14–17]. The low phonon frequency greatly reduces the pairing instability. For the phonon frequency we are using, we find that when the hybridization between the conduction electrons and the localized $4f$ electrons is weak enough, the charge density wave (CDW) instability always dominates, which is consistent with results from the DMFT of the Holstein model [54].

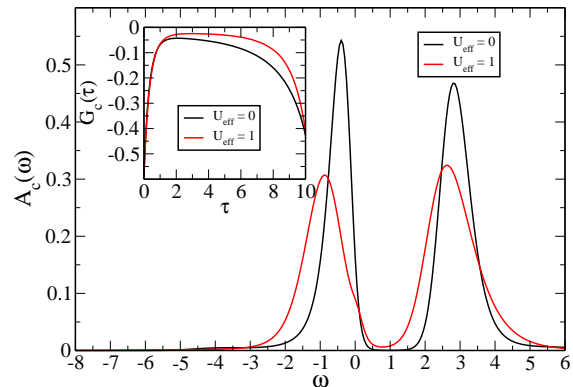


FIG. 3. Main panel: The conduction electrons DOS for $U_{eff} = 0$ and $U_{eff} = 1$ when $V = 1.8, \beta = 10, \Omega_0 = 0.01$. Here, the introduction of the electron-phonon interaction has no significant influence on the DOS, which at the Fermi energy is always finite whether there is electron-phonon interaction or not. Inset: The local $G_c(\tau)$ for small and large electron-phonon interaction strength.

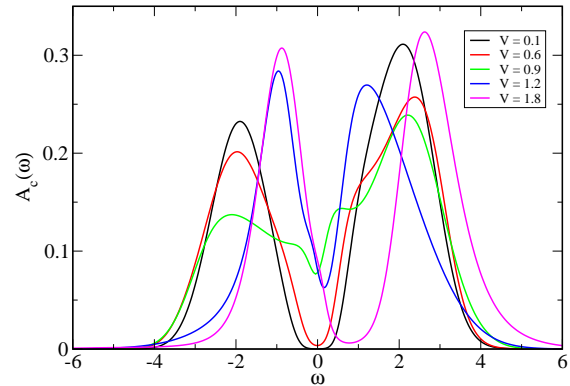


FIG. 4. The c -electron spectral functions for $\beta = 10, \Omega_0 = 0.01, U_{eff} = 1$, at different values of V . When V is small (below 0.6), the electron-phonon interaction dominates over the Kondo screening, and the conduction electrons form a Mott insulator. When V gets large, the Kondo effect dominates over the electron-phonon interaction effect, and the conduction electrons become metallic.

The opening of the Mott gap at the Fermi level is present only when the hybridization between conduction band and localized electrons is weak compared with the electron-phonon coupling. Fig. 3 shows that when the hybridization is strong, the opening of the Mott gap is prohibited. In this parameter regime, the introduction of the electron-phonon interaction has little effect on the behavior of the conduction electron DOS. Since the filling number of the c -electrons is set to 0.8, the hybridization cannot induce a gap at the Fermi energy [55], and thus the DOS is always finite irrespective whether there is electron-phonon interaction or not. Consequently, the c -electrons are always metallic in the large V regime.

The absence of the Mott gap in the large V regime signals that the electron-phonon interaction effect is suppressed by the hybridization. Since the electron charge susceptibility is positively correlated with U_{eff} , the suppression of the electron-phonon coupling effect is also reflected in the decrease of the charge susceptibility as V increases for fixed β (not shown). As V increases from 0.1 to 1.8, the localized f electron moments that are present at small V get screened by the conduction electrons when V is large [32]. At the same time, the conduction electrons make a transition from insulator to metal. The c -electron spectral functions for $\beta = 10$ and $U_{eff} = 1$ with varying values of V are shown in Fig. 4, where a gap at the Fermi energy is clearly visible for $V < 0.6$. When $V > 0.6$, the Mott gap evolves into a depression which disappears completely for $V > 1.2$. Therefore the Mott metal-insulator transition is present only when the electron-phonon interaction is strong enough.

IV. CONCLUSION

In conclusion, using the periodic Anderson model with phonon coupled to the conduction band, and by introducing a volume and temperature dependent bulk modulus contribution to the total pressure, we find a first order phase transition which can explain the volume collapse transitions. A prominent example of volume collapse transition is the $\gamma \rightarrow \alpha$ transition of Cerium. We find that the volume collapse transition of our model is enhanced by the presence of the electron-phonon interaction; with other parameters being fixed we do not find the first order transition for much lower temperature in the absence of the electron-phonon interaction. Recent experiments have shown the phonon plays an important role in the volume collapse transition in Cerium. Our finding supports that the electron-phonon coupling can enhance the first order phase transition.

Moreover, we find that our model, although originally conceived with the Kondo volume collapse scenario in

mind, exhibits interesting features of the metal to insulator transition, e.g., a gap at the Fermi energy in the conduction electrons opens at low temperature, and it is proportional to the effective electron-phonon interaction, U_{eff} .

An obvious improvement over the present work is to include other contributions to the model. The spin orbit coupling and the hybridization in the f-band can be considered in the DMFT calculation, however a more realistic electron-phonon coupling will be beyond the formalism of DMFT and will require a numerical method which can handle long range coupling properly.

Acknowledgements. This material is based upon work supported by the National Science Foundation under the NSF EPSCoR Cooperative Agreement No. EPS-1003897 with additional support from the Louisiana Board of Regents. Computer support is provided by the Louisiana Optical Network Initiative, and by HPC@LSU computing. MJ was also supported by the NSF Materials Theory grant DMR1728457.

-
- [1] A. W. Lawson and T.-Y. Tang, Phys. Rev. **76**, 301 (1949).
 - [2] B. Johansson, Philos. Mag. **30**, 469 (1974).
 - [3] J. W. Allen and R. M. Martin, Phys. Rev. Lett. **49**, 1106 (1982).
 - [4] K. Held, C. Huscroft, R. Scalettar, and A. McMahan, Phys. Rev. Lett. **85**, 373 (2000).
 - [5] K. Held, A. McMahan, and R. Scalettar, Phys. Rev. Lett. **87**, 276404 (2001).
 - [6] L. Z. Liu, J. W. Allen, O. Gunnarsson, N. E. Christensen, and O. K. Andersen, Phys. Rev. B **45**, 8934 (1992).
 - [7] A. K. McMahan, K. Held, and R. T. Scalettar, Phys. Rev. B **67**, 075108 (2003).
 - [8] A. P. Murani, Z. A. Bowden, A. D. Taylor, R. Osborn, and W. G. Marshall, Phys. Rev. B **48**, 13981 (1993).
 - [9] C. R. Burr and S. Ehara, Phys. Rev. **149**, 551 (1966).
 - [10] M. Jarrell, Phys. Rev. Lett. **69**, 168 (1992).
 - [11] A. Georges and G. Kotliar, Phys. Rev. B **45**, 6479 (1992).
 - [12] T. Pruschke, D. L. Cox, and M. Jarrell, Phys. Rev. B **47**, 3553 (1993).
 - [13] A. V. Nikolaev and A. V. Tsvyashchenko, Physics-Uspekhi **55**, 657 (2012).
 - [14] F. Decremps, D. Antonangeli, B. Amadon, and G. Schmerber, Phys. Rev. B **80**, 132103 (2009).
 - [15] M. Krisch, D. Farber, R. Xu, D. Antonangeli, C. Aracne, A. Beraud, T.-C. Chiang, J. Zarestky, D. Y. Kim, E. I. Isaev, et al., Proc. Natl. Acad. Sci. U.S.A. **108**, 9342 (2011).
 - [16] B. Amadon, S. Biermann, A. Georges, and F. Aryasetiawan, Phys. Rev. Lett. **96**, 066402 (2006).
 - [17] I.-K. Jeong, T. W. Darling, M. J. Graf, T. Proffen, R. H. Heffner, Y. Lee, T. Vogt, and J. D. Jorgensen, Phys. Rev. Lett. **92**, 105702 (2004).
 - [18] M. Casadei, X. Ren, P. Rinke, A. Rubio, and M. Scheffler, Phys. Rev. B **93**, 075153 (2016).
 - [19] M. Casadei, X. Ren, P. Rinke, A. Rubio, and M. Scheffler, Phys. Rev. Lett. **109**, 146402 (2012).
 - [20] K. Haule, V. Oudovenko, S. Y. Savrasov, and G. Kotliar, Phys. Rev. Lett. **94**, 036401 (2005).
 - [21] B. Chakrabarti, M. E. Pezzoli, G. Sordi, K. Haule, and G. Kotliar, Phys. Rev. B **89**, 125113 (2014).
 - [22] N. Lanatà, Y.-X. Yao, C.-Z. Wang, K.-M. Ho, J. Schmalian, K. Haule, and G. Kotliar, Phys. Rev. Lett. **111**, 196801 (2013).
 - [23] S. V. Streltsov, A. O. Shorikov, and V. I. Anisimov, JETP Letters **92**, 543 (2010).
 - [24] B. Amadon and A. Gerossier, Phys. Rev. B **91**, 161103 (2015).
 - [25] B. Amadon, J. Phys. Condens. Matter **24**, 075604 (2012).
 - [26] B. Amadon and A. Gerossier, Phys. Rev. B **91**, 161103 (2015).
 - [27] B. Amadon, Phys. Rev. B **94**, 115148 (2016).
 - [28] M.-F. Tian, H.-F. Song, H.-F. Liu, C. Wang, Z. Fang, and X. Dai, Phys. Rev. B **91**, 125148 (2015).
 - [29] N. Devaux, M. Casula, F. Decremps, and S. Sorella, Phys. Rev. B **91**, 081101 (2015).
 - [30] R. Dong, X. Wan, X. Dai, and S. Y. Savrasov, Phys. Rev. B **89**, 165122 (2014).
 - [31] B. Amadon, T. Applencourt, and F. Bruneval, Phys. Rev. B **89**, 125110 (2014).
 - [32] P. Zhang, P. Reis, K.-M. Tam, M. Jarrell, J. Moreno, F. Assaad, and A. K. McMahan, Phys. Rev. B **87**, 121102 (2013).
 - [33] W. Nolting, G. G. Reddy, A. Ramakanth, D. Meyer, and J. Kienert, Phys. Rev. B **67**, 024426 (2003).
 - [34] R. Peters and T. Pruschke, Phys. Rev. B **76**, 245101 (2007).
 - [35] A. Koga, N. Kawakami, R. Peters, and T. Pruschke, Phys. Rev. B **77**, 045120 (2008).
 - [36] A. Koga, N. Kawakami, R. Peters, and T. Pruschke, Journal of the Physical Society of Japan **77**, 033704 (2008).
 - [37] A. Georges, G. Kotliar, W. Krauth, and M. J. Rozenberg, Rev. Mod. Phys. **68**, 13 (1996).

- [38] F. F. Assaad and T. C. Lang, Phys. Rev. B **76**, 035116 (2007).
- [39] W. E. Pickett, A. J. Freeman, and D. D. Koelling, Phys. Rev. B **23**, 1266 (1981).
- [40] R. Podloucky and D. Glötzl, Phys. Rev. B **27**, 3390 (1983).
- [41] M. Jarrell and J. E. Gubernatis, Phys. Rep. **269**, 133 (1996).
- [42] L. de' Medici, A. Georges, G. Kotliar, and S. Biermann, Phys. Rev. Lett. **95**, 066402 (2005).
- [43] K. Mielson, E. Khatami, D. Galanakis, A. Macridin, J. Moreno, and M. Jarrell, Phys. Rev. B **80**, 140505 (2009).
- [44] A. McMahan, C. Huscroft, R. Scalettar, and E. Pollock, J. Comput. Aided Mater. Des. **5**, 131 (1998).
- [45] J. R. Schrieffer and P. A. Wolff, Phys. Rev. **149**, 491 (1966).
- [46] R. Grover, I. C. Getting, and G. C. Kennedy, Phys. Rev. B **7**, 567 (1973).
- [47] F. Murnaghan, Proc. Natl. Acad. Sci. U.S.A. **30**, 244 (1944).
- [48] P. Yu, R. Wang, D. Zhao, and H. Bai, App. Phys. Lett. **91**, 201911 (2007).
- [49] K. Moore, L. Belhadi, F. Decremps, D. Farber, J. Bradley, F. Occelli, M. Gauthier, A. Polian, and C. Aracne-Ruddle, Acta Mater. **59**, 6007 (2011).
- [50] D. Meyer, A. Hewson, and R. Bulla, Phys. Rev. Lett. **89**, 196401 (2002).
- [51] Q. Si, G. Kotliar, and A. Georges, Phys. Rev. B **46**, 1261 (1992).
- [52] J. Freericks and V. Zlatić, Rev. Mod. Phys. **75**, 1333 (2003).
- [53] E. Müller-Hartmann, Z. Phys. B **76**, 211 (1989).
- [54] J. Freericks, M. Jarrell, and D. Scalapino, Phys. Rev. B **48**, 6302 (1993).
- [55] T. Pruschke, R. Bulla, and M. Jarrell, Phys. Rev. B **61**, 12799 (2000).